

a reprint from Applied Optics

Infrared polarization signature from cirrus clouds

Y. Takano and K. N. Liou

The authors are with the Department of Meteorology/
Center for Atmospheric and Remote Sounding Studies,
University of Utah, Salt Lake City, Utah 84112.

Received 6 May 1991.

0003-6935/92/121916-04\$05.00/0.

© 1992 Optical Society of America.

Maximum infrared polarization signature of up to 1% is predicted in tropical subvisual cirrus involving randomly oriented ice crystals, based on radiative transfer calculations.

Key words: cirrus infrared polarization

In the development of target detection based on the infrared signature from space, air, and the ground, the effects of cirrus clouds, particularly subvisual cirrus, on infrared transmission must be understood. The radiative properties of cirrus clouds have been investigated by Takano and Liou,^{1,2} who used the scattering and absorption data derived from hexagonal ice crystals. They specifically developed the radiative transfer method has been for solar wavelengths in

which thermal emission can be neglected. Liou *et al.*³ extended the radiative transfer methodology to thermal infrared wavelengths in order to study the transmission properties of thin cirrus clouds. In Ref. 1 we demonstrated that there are important polarization signatures of reflected sunlight from clouds. These signatures could be used to differentiate between spherical and nonspherical particles as well as to distinguish among various nonspherical particles.

However, the information content of the polarization from cirrus clouds in the thermal infrared wavelengths has not been explored. The contribution to sky polarization from hexagonal and oriented ice crystals could be significant. It is our objective in this Note to present some results regarding the radiance and polarization patterns for the 10- μm wavelength in a number of cirrus-cloudy atmospheres.

The single-scattering properties for randomly oriented hexagonal ice crystals in the infrared wavelengths have been computed with the program developed by Takano and Liou.¹ Figure 1(a) shows the phase function for hexagonal ice crystals with an aspect ratio ($L/2a$) of 120/60 ($\mu\text{m}/\mu\text{m}$) at the 10- μm wavelength, where L is the length and $2a$ is

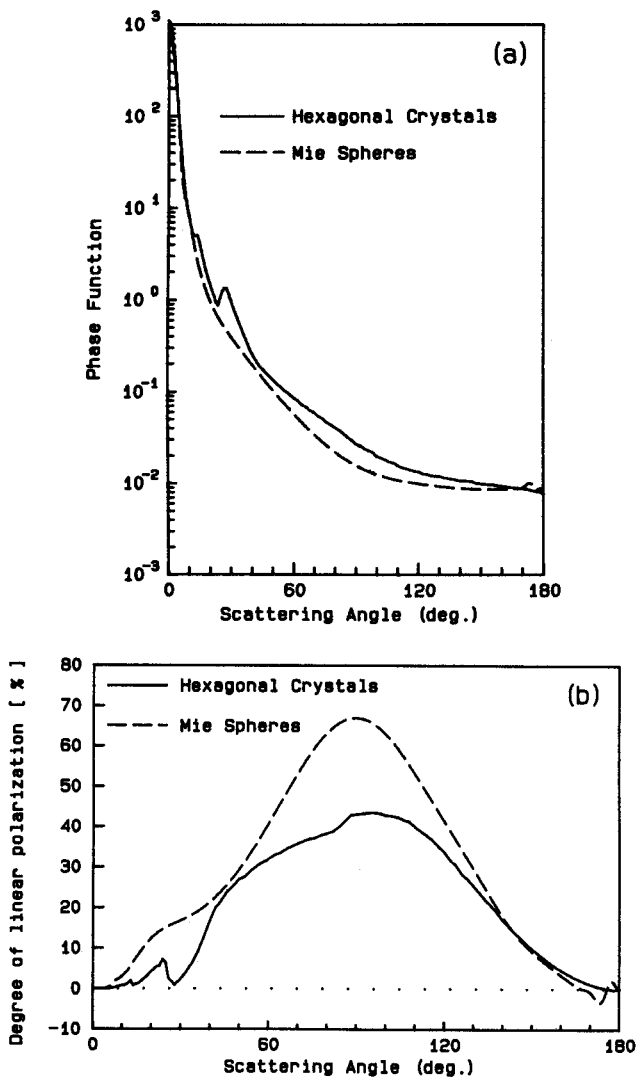


Fig. 1. (a) Scattering phase function and (b) degree of linear polarization for randomly oriented hexagonal ice crystals of $L/2a = 120/60$ ($\mu\text{m}/\mu\text{m}$) and the area equivalent Mie spheres at $\lambda = 10 \mu\text{m}$.

the width of a hexagonal crystal. The complex refractive index of ice⁴ used in this computation is $1.1991 - j0.051$. For comparison, the phase function for the area-equivalent Mie spheres is also shown in Fig. 1(a). The peaks on the ice crystal phase function at the scattering angles of 14° and 27° correspond, respectively, to inner and outer halos, which are at different angles from the standard 22° and 46° halos in the visible because of the differences in refractive indices. Ice crystals scatter more light in backward directions than do spheres. Figure 1(b) shows the degree of linear polarization that is due to single scattering of hexagonal crystals and spheres. Generally, the degree of linear polarization for hexagonal crystals is smaller than that for ice spheres. Using the single-scattering and polarization data, we carried out computations of the transfer of polarized infrared radiation in cirrus-cloudy atmospheres. Under plane-parallel conditions, radiance and polarization patterns are azimuthally independent. They are functions only of the optical depth and zenith angle. In the computations the surface is assumed to emit unpolarized radiation isotropically.

We used tropical midlatitude winter and arctic winter atmospheric profiles in performing the radiance and polarization calculations. The cloud and surface temperatures for these profiles, which are of prime importance in infrared radiative transfer calculations, are listed in Table I. The heights of the cirrus clouds are also included in this table. We used a columnar ice crystal shape with an aspect ratio (length/diameter) of $120/60$ ($\mu\text{m}/\mu\text{m}$), whose single-scattering properties at $10 \mu\text{m}$ are shown in Fig. 1.

Figure 2 shows the upward radiances at the cloud top and the downward radiances at the cloud base. Limb darkening and limb brightening are evident in upward and downward patterns, respectively. These patterns can also be seen in the window radiances.⁵ When the cloud optical depth is small ($\tau_c = 1$), the upward radiance for zenith angles less than $\sim 60^\circ$ are close to those emitted from the surface. For zenith angles larger than $\sim 60^\circ$, the upward radiance is reduced because of cloud absorption of the radiation emitted from the surface. However, the downward radiance is enhanced as a result of the combined effects of cloud emission and the cloud reflection of surface radiation. The upward radiances decrease with an increase in optical depth in any models, because cirrus clouds absorb the radiation emitted by a surface. In contrast, the downward radiances increase with an increase in optical depth in any models, because of the emission of cirrus clouds. When the cloud optical depth is large ($\tau_c = 4$), the downward radiances for zenith angles less than $\sim 60^\circ$ are close to those emitted from the cloud. As Fig. 2 shows, radiance patterns depend on the atmospheric temperature profile used in the calculation. For $\tau_c = 1$ the upward radiances increase relative to the surface temperature. Exceptions are for the tropical case involving zenith angles greater than $\sim 70^\circ$ because of the lower temperature of the tropical anvil. For optically thick clouds with $\tau_c = 4$, the upward radiances are produced largely by the cloudtop emission. The downward radiances depend primarily on the cloud temperature.

The degree of linear polarization⁶ patterns corresponding to Fig. 2 is illustrated in Fig. 3. Because of the differences in upward and downward radiances, the linear polarization patterns are also different at the top and base of the cloud. There is a significant difference in linear polarization patterns between thermal infrared and solar wavelengths. The magnitude of linear polarization displayed in Fig. 3, which is generally less than 1%, is much smaller than that in the case of solar radiation (see Fig. 8 of Ref. 2). This is so because the surface and a small volume of cloud are assumed to emit unpolarized thermal radiation isotropically. We shall consider the optically thin case ($\tau_c = 1$) in Figs. 3(a) and 3(b), in which the effect of single-scattering events on polarization is most pronounced. In this case, radiation that emerges from the cloud top is dominated by the emission from the surface and is largely unpolarized for zenith angles less than 60° . For larger zenith angles,

Table I. Cloud and Surface Temperature and Cloud Heights for Three Atmospheric Profiles

Profile	Cloud Height (km)	Cloud Temperature, T_c (K)	Surface Temperature, T_s (K)
Tropical	~ 15.0	200	300
Midlatitude Winter	~ 8.0	230	272
Arctic Winter	~ 6.5	227	257

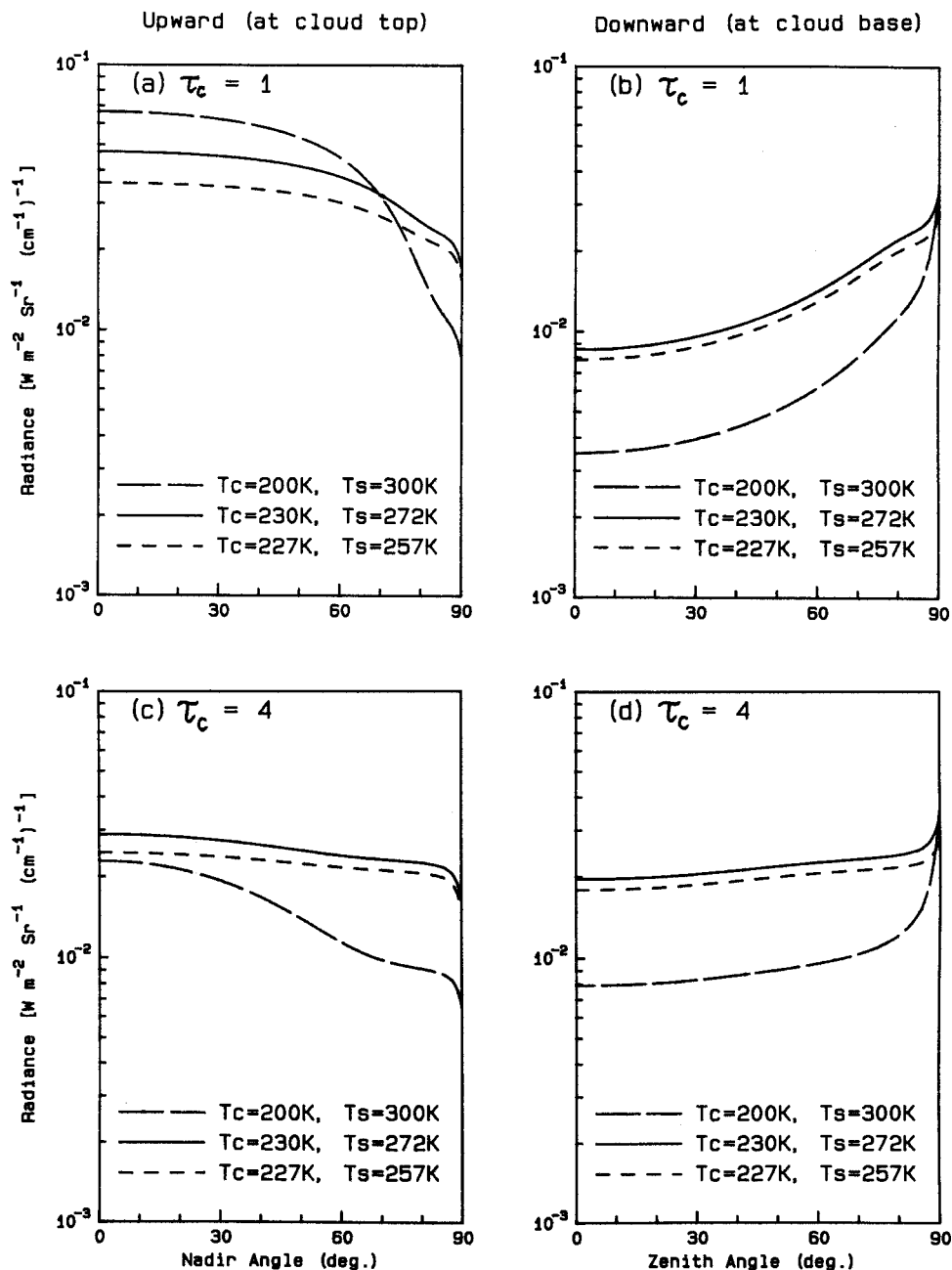


Fig. 2. Radiances as a function of zenith/nadir angles on the boundaries of cirrus clouds in the three atmospheric profiles in the cases of (a), (b) $\tau_c = 1$ and (c), (d) $\tau_c = 4$.

positive polarization may be produced by single scattering of the emitted unpolarized radiation from the surface, as illustrated in Fig. 1(b). At the cloud base, positive linear polarization is also produced as a result of the single scattering of the emitted unpolarized radiation from the surface. When τ_c is $1/8$, downward polarization can reach more than 1% at $\theta \approx 60^\circ$. When the cloud's optical depth increases, polarization that is produced by single scattering is generally reduced. However, total polarization does not depend monotonically on optical depth, because of the combined effect of radiances from the cloud and the surface.

From Figs. 3(a) and 3(c) it can be generally concluded that the upward polarization at the top of clouds composed of randomly oriented ice crystals is small, and, for all practical purposes, the polarization can be neglected. In the

case of downward components, polarization that emerges from the tropical cirrus is greater than that which emerges from midlatitude and arctic cirrus by approximately an order of magnitude, as Figs. 3(b) and 3(d) show. This phenomenon can be explained as follows: First, consider only a cirrus cloud without an underlying surface. The degree of linear polarization at the cloud boundaries is slightly negative and is independent of the cloud temperature. This is because the effect of cloud temperature is canceled out in the denominator and the numerator of $-Q/I$. Second, we add a surface below a thin cirrus cloud. The total polarization is largely affected by the single scattering of surface-emitted radiation by ice crystals. Generally, single-scattered radiation has a positive linear polarization, as was pointed out by Fig. 1. The temperature

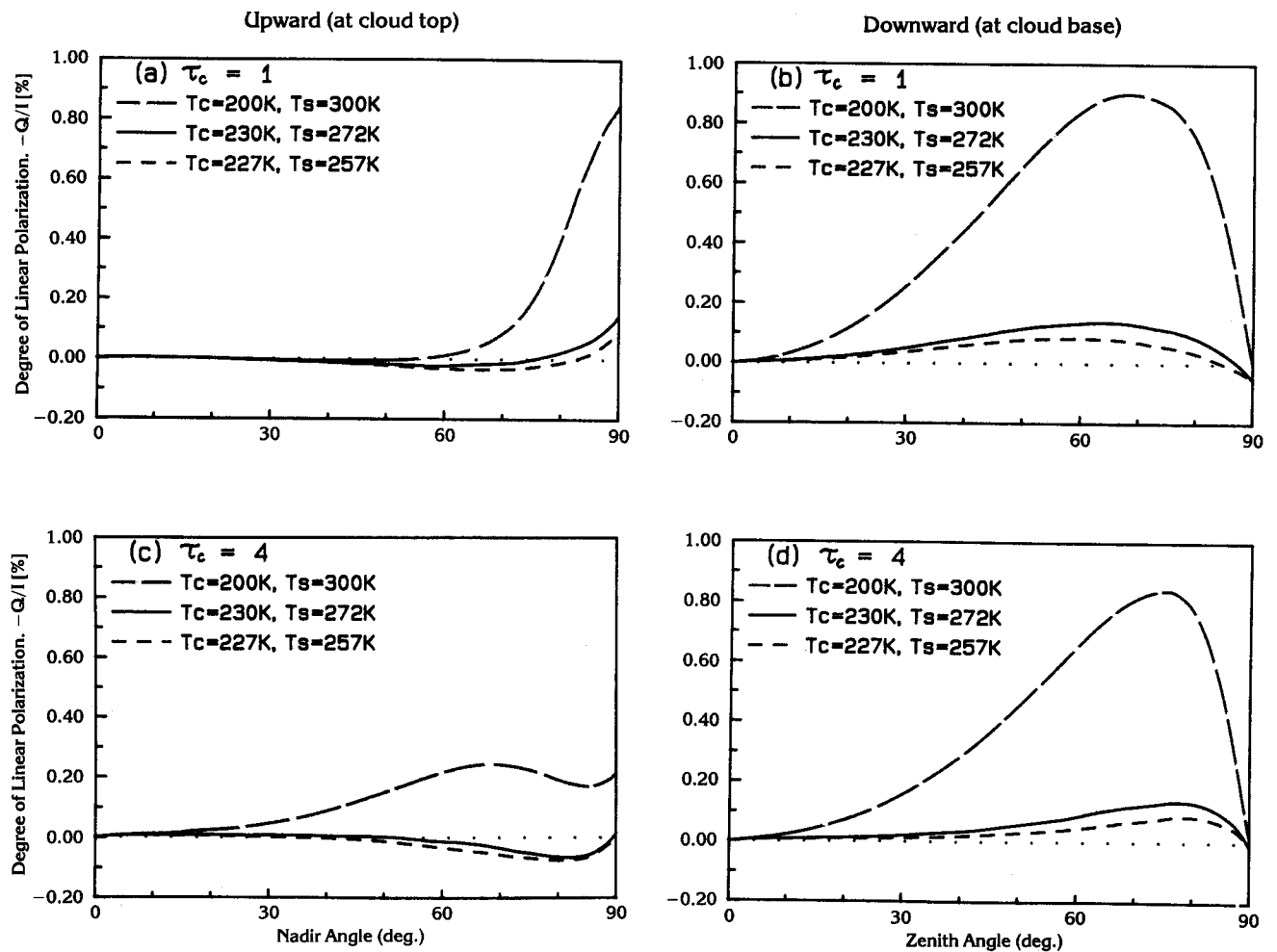


Fig. 3. Degree of linear polarization as a function of zenith/nadir angles on the boundaries of cirrus clouds in the three atmospheric profiles in the cases of (a), (b) $\tau_c = 1$ and (c), (d) $\tau_c = 4$.

difference between the surface and the cloud in the case of tropical cirrus is greater than that for the midlatitude and arctic cirrus. As a result, the tropical cirrus cloud shows more intense positive polarization than the midlatitude and arctic cirrus. Downward polarization for water clouds will also be small because of the smaller differences between surface and cloud temperatures.

Radiance and polarization patterns have also been calculated for ice plates with an aspect ratio of 20/20 ($\mu\text{m}/\mu\text{m}$). Computed results are close to those for ice columns with an aspect ratio of 120/60 ($\mu\text{m}/\mu\text{m}$). The radiance and the degree of linear polarization at the cirrus cloud boundaries depend more on the difference between the surface and cloud temperatures than on the cloud particle size and shape. Downward infrared polarization at the cloud base in the case of tropical cirrus can reach more than 1%, which is greater than that for the cases of midlatitude and arctic cirrus by approximately an order of magnitude. At the wavelength of 10 μm , optical depths of air molecules and aerosols are small. Thus detection of tropical subvisual cirrus may be possible by measuring downward polarization at zenith angles of 60°–70° from the surface. This possibility will be explored in our future research efforts. The effects of horizontal orientation of ice crystals, and associated anisotropic emission, on infrared polarization are also subjects for further investigation.

This work has been supported by the U.S. Office of Naval Technology through the Naval Air Development Center under contract N62269-89-C-0561. A part of the computations contained in this research work has been carried out on the San Diego supercomputer, Cray Y-MP 8/864. We thank M. Hess for helpful comments on this Note.

References

1. Y. Takano and K. N. Liou, "Solar radiative transfer in cirrus cloud. Part I: Single-scattering and optical properties of hexagonal ice crystals," *J. Atmos. Sci.* **46**, 3–19 (1989).
2. Y. Takano and K. N. Liou, "Solar radiative transfer in cirrus clouds. Part II. Theory and computation of multiple scattering in an anisotropic medium," *J. Atmos. Sci.* **46**, 20–36 (1989).
3. K. N. Liou, Y. Takano, S. C. Ou, A. J. Heymsfield, and W. Kreiss, "Infrared transmission through cirrus clouds: A radiative model for target detection," *Appl. Opt.* **29**, 1886–1896 (1990).
4. S. Warren, "Optical constants of ice from the ultraviolet to the microwave," *Appl. Opt.* **23**, 1206–1225 (1984).
5. K. N. Liou, "On the radiative properties of cirrus in the window region and their influence on remote sensing of the atmosphere," *J. Atmos. Sci.* **31**, 522–532 (1974).
6. K. N. Liou, *An Introduction to Atmospheric Radiation* (Academic, New York, 1980), Chap. 3, p. 81.

Relationship between backscattering and extinction coefficients of aerosols with application to turbid atmosphere: erratum

K. Parameswaran, K. O. Rose, and B. V. Krishna Murthy

The authors are with the Space, Physics Laboratory, Vikram Sarabhai Space Centre, Trivandrum 695 022, India.

Received 22 November 1991.

0003-6935/92/121920-01\$05.00/0.

© 1992 Optical Society of America.

Equations (11) and (12) of our recent paper¹ should read as follows:

$$\beta = \exp[C_0(1 + uR^{-v})]\alpha^{k_0(1-pR^{-q})}, \quad (11)$$

$$\beta = \exp(C_0)\alpha. \quad (12)$$

Reference

1. K. Parameswaran, K. O. Rose, and B. V. Krishna Murthy, "Relationship between backscattering and extinction coefficients of aerosols with application to turbid atmosphere: erratum," *Appl. Opt.* 30, 3059-3071 (1991).